J Mater Sci (2008) 43:2675–2679
DOI 10.1007/s10853-007-2436-6

Doping effects of structural transformation and soft mode in $Ba_xPb_{1-x}TiO_3$ nanoparticles

C. T. Lee · M. S. Zhang · Z. Yin

Received: 6 September 2007 / Accepted: 27 December 2007 / Published online: 19 February 2008

Abstract $Ba_xPb_{1-x}TiO_3$ nanoparticles with various Ba concentrations were synthesized by stearic acid method. Structural transformation, ferroelectricity, and soft mode character under various Ba concentrations were examined by X-ray diffraction, differential scanning calorimetry, and Raman spectroscopy. When the Ba concentration in $Ba_xPb_{1-x}TiO_3$ nanoparticle increases, tetragonality c/a reduces, transition temperature T_c decreases and the E(1TO) soft mode softens. A critical Ba doping concentration of $x = 0.4$ was found. Above the concentration tetragonality c/a reaches ~ 1 and ferroelectricity disappears, and the E(1TO) soft mode also vanishes. Differential scanning calorimetric measurement on heating and cooling shows small thermal hysteresis $\Delta T = 4$ °C in $Ba_xPb_{1-x}TiO_3$ nanoparticle which manifests a weak first-order transition of the specimen. On the basis of the different electronic structures of Ba and Pb atoms, the mechanisms of the doping effects of ferroelectricity, structural transformation, and phonon properties are discussed and attributed to decrease in hybridization between Ti 3*d* and O 2*p* states via indirect interaction between the Ba 5*p* and O 2*p* states.

Introduction

$Ba_xPb_{1-x}TiO_3$ (BPTO) nanoparticles have been received much attention for both technical and fundamental research sides. On the technical applications they can be made as thermostat elements, ambient thermal state indicators etc. On the fundamental research there are rather interesting matters such as phase transformation and lattice dynamics to be studied [1–6]. It is well known that $PbTiO_3$ belongs to a ferroelectric material with strong ferroelectricity for its large strain of 6% ($c/a = 1.06$), while $BaTiO_3$ is of weak ferroelectricity for its small strain of 1% ($c/a = 1.01$) [7]. It is interesting to know the Ba doping dependence on ferroelectricity, structural transformation and phonon characters in $Ba_xPb_{1-x}TiO_3$ nanoparticle, which seems to be alloyed by barium oxide and lead oxide. Such research is helpful to better understand the relationship between lattice dynamics versus the doping in the complex compound. The relative properties can be adjusted by changing the doping content, which is in favor of material designing. There are a number of techniques, such as sol–gel, hydrothermal, solid-state reaction and stearic acid methods to prepare nanoparticles [8–11]. On basis of preparation for $Ba_xPb_{1-x}TiO_3$ (BPTO) nanoparticles with different Ba contents under stearic acid method, X-ray diffraction (XRD), differential scanning calorimetry (DSC) and Raman spectroscopy (RS) were used to examine the Ba concentration effects on ferroelectricity, structural transformation and soft mode properties. Special attention is paid to discussing the origin of Ba doping effects in $Ba_xPb_{1-x}TiO_3$ nanoparticle solid solutions from hybridization effect between Ba and Pb atoms.

Experiment

BPTO nanoparticles were synthesized by stearic acid method with barium stearate, lead stearate and $Ti(C_4H_9O)_4$ as the precursor materials. The preparation procedures

C. T. Lee · M. S. Zhang (✉) · Z. Yin
National Laboratory of Solid State Microstructures, and Center for Materials Analysis, Nanjing University, Nanjing 210093, PR China
e-mail: mszhang@nju.edu.cn

were as follows. Barium stearate and lead stearate were dissolved in molten stearate acid (70 °C). $Ti(C_4H_9O)_4$ was added into the solution with fully mixing. The resulted solutions were gelled at room temperature, and then heated at 400 °C to form $Ba_xPb_{1-x}TiO_3$ powders, which were finally annealed at 800 °C for 1 h to form BPTO nanoparticles.

Morphology of BPTO nanoparticle was observed by JEOL JSM-6300 Scanning Electron Microscope (SEM). XRD patterns were recorded on Rigaku X-ray diffractometer with Cu (α as the incident radiation. Thermal measurement was performed on Perkin-Elmer DSC-2C Differential Scanning Calorimeter with temperature rate by 20 °C/min. Raman spectra were measured on J.Y HR-800 Raman spectrometer, with excitation of 488 nm blue beam and output power of 16 MW.

Results and discussion

Morphology of BPTO nanoparticle was observed by SEM. Since the grain size measurement shows less size dependence on the Ba doping content later, Fig. 1 shows the morphology of BPTO at $x = 0.2$. It can be seen that the most of the particles exhibit uniform sphere-shapes, and some clusters were formed because of the high activity induced by unsaturated atom sites and surface energy [12].

Figure 2 showsXRD patterns of BPTO nanoparticles with Ba contents from $x = 0.1$ to $x = 0.5$. For comparison the pattern of $PbTiO_3$ ($Ba_xPb_{1-x}TiO_3$ at $x = 0$) is also plotted. The averaged particle size can be obtained via Scherrer's equation [13], $D = k\lambda/\beta \cos\theta$, where k is the constant (shape factor about 1.0), λ is the X-ray wavelength (1.542 Å), β the FWHM of the diffraction peak and θ is the

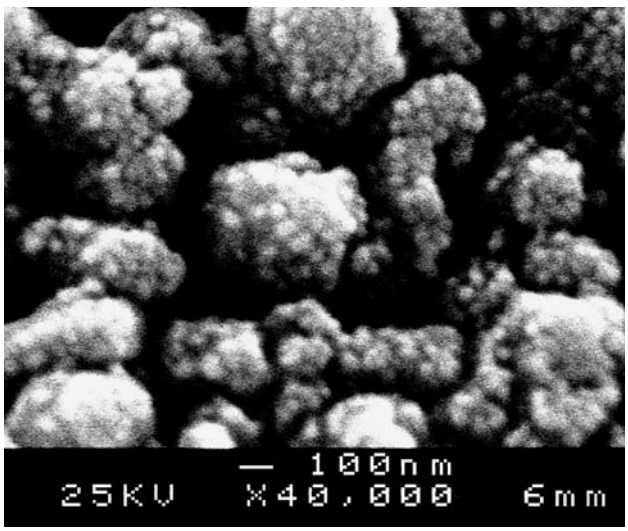

Fig. 1 Morphology of $Ba_xPb_{1-x}TiO_3$ ($x = 0.2$) nanoparticle

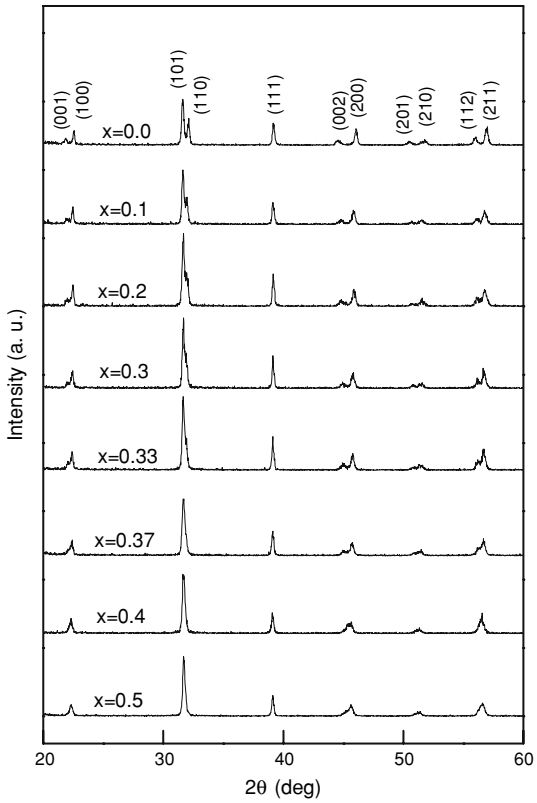

Fig. 2 XRD patterns of $Ba_xPb_{1-x}TiO_3$ nanoparticle at various Ba concentrations

diffraction angle. From the (101) and (110) peaks the averaged particle sizes calculated by Scherrer's equation are 49, 46, 45, 45, 44, 44, and 42 nm for $x = 0$, 0.1, 0.2, 0.3, 0.33, 0.37, and 0.4, respectively. These values indicate that Ba concentration does not make appreciable influence on the particle size. As the Ba doping increases to 0.4, all the peaks of (001), (100), (101), (110), (002), (200), (201), (210), (112) and (211) become peaks of (100), (101), (200), (210) and (211) and peaks of (001), (110), (002), (201) and (112) disappear. This illustrates that at $x = 0.4$ the tetragonal phase (ferroelectric phase) completely transforms into the cubic phase (paraelectric phase), which means that above the critical Ba doping content ($x = 0.4$) the ferroelectric phase vanishes, the ferroelectric–paraelectric transition disappears. It is worthy to note that in addition to contribution from Ba doping to the phase transition, size effect also makes contribution.

Figure 3 depicts the Ba concentration dependence of lattice constants a, c, and the tetragonality c/a of BPTO nanoparticles. It is clearly shown that with increasing Ba content lattice parameter a increases whereas c decreases. This leads to decrease of the ratio of c/a from 1.06 at $x = 0$ to 1.0022 at $x = 0.4$, even much lower than $c/a = 1.01$ for ferroelectric $BaTiO_3$ with weak ferroelectricity [7]. The Ba concentration dependence of the c/a value shows

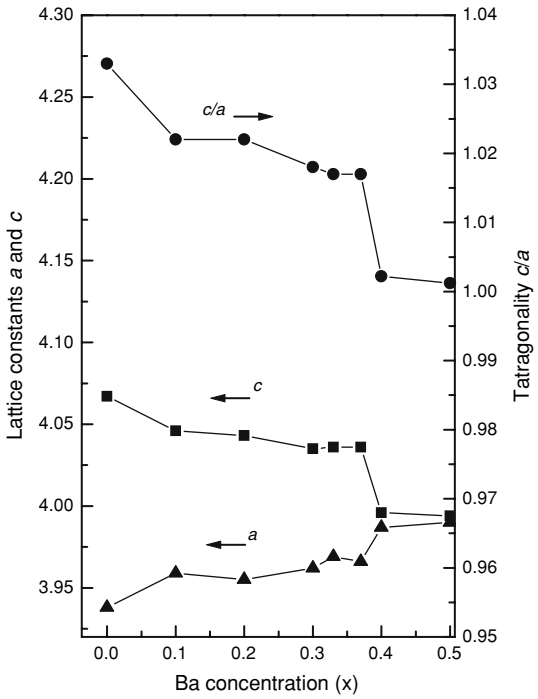

Fig. 3 Tetragonality *c/a* of $Ba_xPb_{1-x}TiO_3$ nanoparticle as a function of Ba concentration

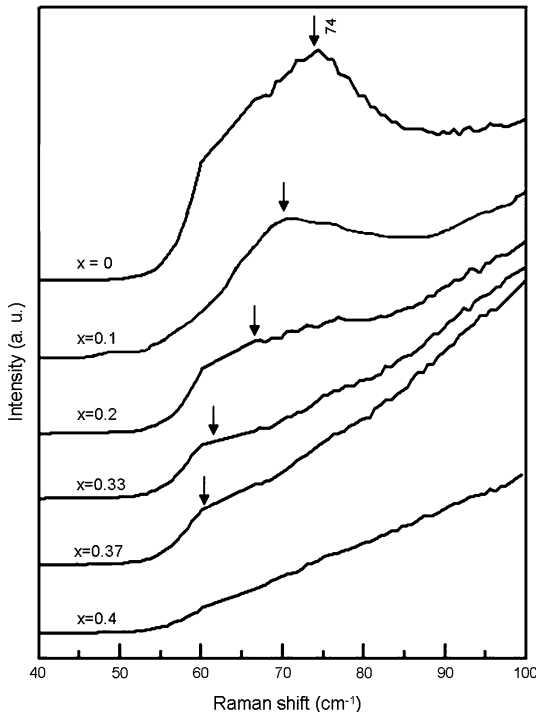

Fig. 4 The E(1TO) soft mode versus Ba concentration in $Ba_xPb_{1-x}TiO_3$ nanoparticle. The arrow shows the E(1TO) soft mode position at different Ba content *x*

that with increasing Ba content BPTO ferroelectricity weakens, and the Ba content reaches $x = 0.4$, the ferroelectricity disappears, that is the ferroelectric–paraelectric transition subsequently vanishes. To elucidate the weakening of ferroelectricity and disappearance of the transition in BPTO nanoparticle, the electronic configurations of BPTO nanoparticles should be discussed. As $x = 0$, BPTO becomes $PbTiO_3$. Pb^{2+} has its electron configuration $4f^{14}5d^{10}6s^2$. Pb 6*s* band locates very close to the O 2*p* bands, and leads to strong hybridization between the Pb 6*s* and O 2*p* states. Thus, the hybridization between the Ti 3*d* and O 2*p* states is indirectly increased, in favor of stabilizing the ferroelectricity, leading to stronger ferroelectricity for $PbTiO_3$ [7, 13]. When Pb^{2+} is partially substituted by Ba^{2+}, less hybridization occurs between the Ba 5*p* and O 2*p* states due to the configuration of the inert gas (Xe) of Ba^{2+} [14]. This means that the interaction between the Ba 5*p* and O 2*p* states indirectly decreases hybridization between the Ti 3*d* and O 2*p* states, causing the weakening of BPTO ferroelectricity, which is consistent with our above XRD results.

Figure 4 shows the E(1TO) soft mode evolution versus Ba content. With increasing Ba concentration, the mode frequency shifts downward and the intensity gradually decreases. Table 1 briefly gives the mode frequencies and intensities at different Ba concentrations. It is clearly shown that the 74 cm^{-1} E(1TO) soft mode at $x = 0$ shifts downward to 62 cm^{-1} at $x = 0.37$, and the intensity

Table 1 E(1TO) soft mode frequency and intensity versus Ba content *x* in $Ba_xPb_{1-x}TiO_3$ nanoparticle

Ba concentration (*x*)	0	0.1	0.2	0.33	0.37	0.4
Frequency (cm^{-1})	74	70	66.5	63	62	–
Intensity	vs	s	ms	w	vw	–

Note: vs, very strong; s, strong; ms, medium-strong; w, weak; vw, very weak

decreases and reaches zero at $x = 0.4$. In comparison with $PbTiO_3$ nanoparticle, the 82 cm^{-1} E(1TO) soft mode shifts to 51 cm^{-1} [15]. These two different results show that Ba doping weakens the softening effect of the E(1TO) mode. In the BPTO bulk, the 89 cm^{-1} E(1TO) mode shifts to 42 cm^{-1} as the Ba concentration increases to $x = 0.7$ [4], and the E(1TO) mode in another BPTO nanoparticle prepared by sol gel technique the 74 cm^{-1} E(1TO) mode shifts to 45 cm^{-1} at $x = 0.7$ [8]. The E(1TO) soft mode shows different softening behaviors in four kinds of samples: E(1TO) mode softens 47 cm^{-1} for bulk BPTO, 31 cm^{-1} for $PbTiO_3$ nanoparticle, 29 cm^{-1} for the 60 nm BPTO nanoparticle prepared by sol gel, and 12 cm^{-1} for our 42 nm BPTO nanoparticle prepared by stearic acid. Those softening behaviors of the soft mode in BPTO sample is obviously owing to the size effect. The smaller

size BPTO nanoparticle shows the weaker softening effect for the soft mode.

Raman spectra at different temperatures for both $PbTiO_3$ ($Ba_xPb_{1-x}TiO_3$, at $x = 0$) and $Ba_xPb_{1-x}TiO_3$ ($x = 0.2$) nanoparticles are shown in Fig. 5a, b, respectively. With increasing temperature, frequency of the E(1TO) soft mode in $PbTiO_3$ nanoparticle decreases from 74 cm^{-1} at room temperature to 62 cm^{-1} at 340 °C and then the mode disappears at 350 °C. Frequency of the E(1TO) soft mode in $Ba_{0.2}Pb_{0.8}TiO_3$ nanoparticle decreases from 68 cm^{-1} at room temperature to 62 cm^{-1} at 280 °C and then disappears at 290 °C. The E(1TO) soft mode was broadened and shifted toward the low-frequency region as the temperature approaches T_c, which indicates that with increasing Ba concentration to 0.2, the corresponding T_c decreases from 350 to 290 °C, which is ascribed to the decrease in tetragonality of *c*/*a* by Ba doping. The T_c of 290 °C in our $Ba_xPb_{1-x}TiO_3$ ($x = 0.2$) nanoparticle sample is even lower than that ($T_c = 340$ °C) of $Ba_xPb_{1-x}TiO_3$ ($x = 0.4$) nanoparticle from Ref. [8], such weaker ferroelectricity is attributed to smaller tetragonality *c*/*a*, in smaller nanoparticle size (42 nm) in our BPTO nanoparticle than theirs (60 nm).

DSC curves of BPTO nanoparticles at various Ba concentrations are recorded in Fig. 6. Upon heating and cooling phase transitions occur at temperatures of 345, 283, and 243 °C and 341, 279, and 239 °C for $x = 0$, 0.2, and 0.3, respectively. Decrease in transition temperature with increasing Ba concentration is consistent with our XRD and spectroscopic results. The obtained thermal hysteresis ΔT equals 4 °C in the Ba doping range from $x = 0$ to 0.3. Comparing a strong first-order ferroelectric transition for $PbTiO_3$ crystal, such a small thermal hysteresis shows that the phase transition in BPTO nanoparticle belongs to a weak first-order. The latent heat was calculated to be 0.682, 0.451, and 0.294 kJ/mol for $x = 0$, 0.2, and 0.3, respectively. When $x = 0.4$ both endothermic and exothermic curves become flat and their peaks disappear. DSC data indicate that Ba doping weakens the cubic–tetragonal transition and the transition disappears at the critical Ba concentration $x = 0.4$. The origin is owing to the decrease in hybridization between the Ti 3*d* and O 2*p* states via indirect interaction between the Ba 5*p* and O 2*p* states.

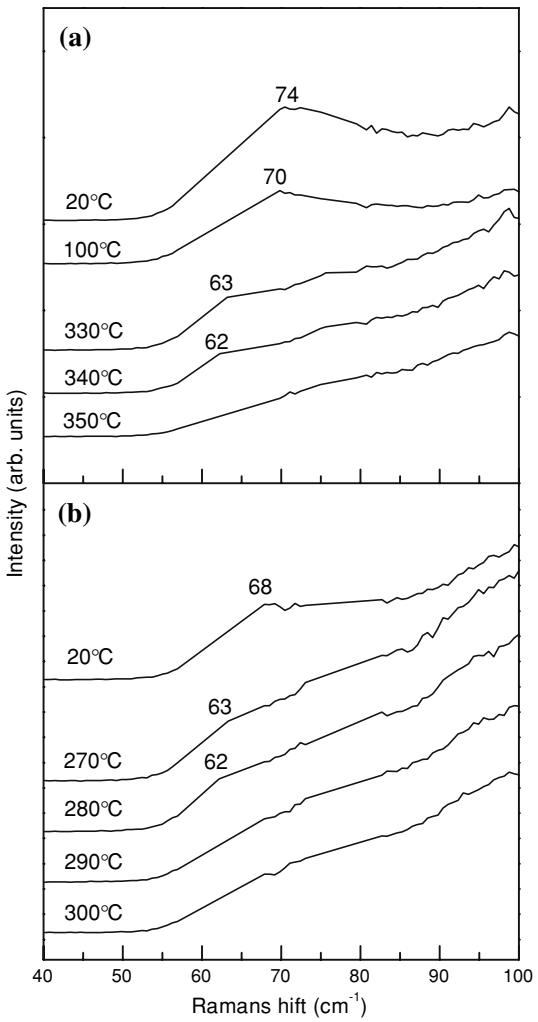

Fig. 5 (**a**) Raman spectra of $PbTiO_3$ nanoparticle and (**b**) Raman spectra of $Ba_xPb_{1-x}TiO_3$ ($x = 0.2$) nanoparticle at various temperatures

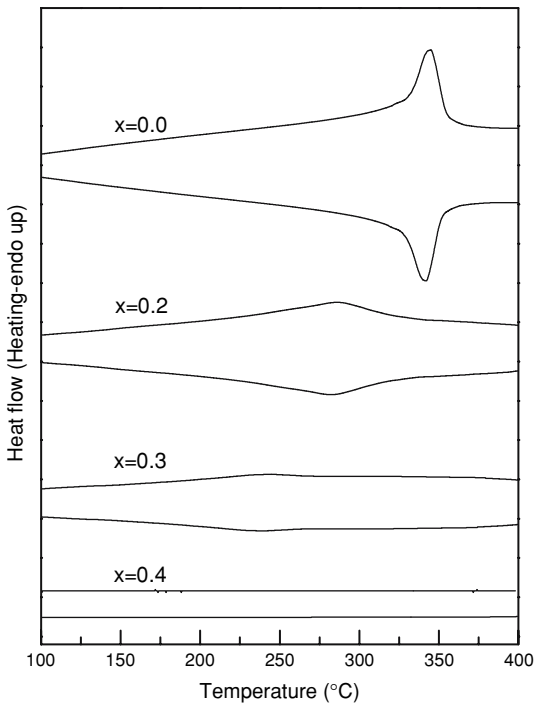

Fig. 6 DSC curves of $Ba_xPb_{1-x}TiO_3$ nanoparticle at different Ba contents with temperature rate of 20 °C/min

Conclusion

We have successfully synthesized BPTO nanoparticles by the stearic acid method. The ferroelectricity, structural transformation and soft mode properties at different Ba concentrations were examined by SEM, XRD, RS, and DSC. With increasing Ba content in BPTO nanoparticle the ferroelectricity is weakened, structural transformation temperature is decreased and the E(1TO) soft mode is softened. A critical Ba doping concentration of $x = 0.4$ was found. The Ba doping effects of ferroelectricity, structural transformation and the E(1TO) soft mode in BPTO nanoparticle are discussed and attributed to decrease in hybridization between the Ti 3*d* and O 2*p* states via indirect interaction between the Ba 5*p* and O 2*p* states. Small thermal hysteresis from DSC measurement indicates a weak first-order phase transition for BPTO nanoparticle.

Acknowledgements The work was supported by the National Natural Science Foundation of China through Grants 10174034 and 10374047.

References

1. Sheng JY (1984) J S&T Inform 2:16
2. Chen WP, Li LT, Gui ZL, Jian Q (1997) J Inorg Mater 12:620
3. Sheng NY, Sun TN, Yu SM, Zhang C (2000) The technology of modern electronic materials. XinHua Press, Beijing
4. Burns G, Scott BA (1971) Solid State Commun 9:813
5. Belous AG, Vyunov OI, Kovalenko LL, Buscaglia V, Viviani M, Nanni P (2003) Inorg Mater 39:133
6. Godefroy G, Jannot B, Michel-Calendini FM (1991) Phase Transit 33:4
7. Cohen RE (1992) Nature 358:137
8. Meng JF, Katiyar RS, Zou GT (1998) J Phys Chem Solids 59:1161
9. Wang XH, Zhao C, Wang Z, Zhao MY (1994) J Alloys Compd 204:33
10. Ren TL, Zhang PL, Zhong WL, Wang XH, Xu BK (1994) Chin Phys Lett 11:310
11. Meng JF, Li JP, Zou GT, Wang XH, Wang ZC, Zhao MY (1994) Chin Phys Lett 11:345
12. Zhang LD, Mo JM (2001) Nanometer materials and nanometer structures, science. Publishing Press, Beijing
13. Cohen RE, Krakauer H (1992) Ferroelectrics 136:65
14. Godefroy G, Jannot B, Michel-Calendini FM (1991) Phase Transit 33:3
15. Ishikawa K, Yoshikawa K, Okada N (1988) Phys Rev B 37:5853